

## Interplay of reaction and transport in a perfect fluid

Damián H. Zanette

*Centro Atómico Bariloche and Instituto Balseiro, Consejo Nacional de Investigaciones Científicas y Técnicas  
8400 Bariloche, Río Negro, Argentina*

(Received 15 February 1994)

The dynamics of a reacting perfect fluid immersed in a background host medium is modeled and studied in several particular situations. Reaction events—which involve interaction of fluid particles with themselves and with the background—are described by a density dependent source term in the mass continuity equation. Mechanical interaction with the background introduces additional terms in the continuity equations for momentum and energy. We analyze the effect of reaction events in sound propagation and study the appearance of nonequilibrium structures, such as wave fronts, paying particular attention to the consequences of the combined action of transport and reaction processes. We also develop a numerical discrete velocity model for the simulation of the reacting fluid, which can be used for comparison with the analytical results.

PACS number(s): 05.60.+w, 47.10.+g, 47.54.+r, 47.70.Fw

### I. INTRODUCTION

The dynamics of physicochemical systems whose components undergo transport processes and interact through reaction events—during which they are “created” or “annihilated”—has been the subject of a great amount of work during the past two decades (see, for instance, Ref. [1] and references therein). Besides their obvious interest in many applications [2,3], such systems are paradigmatic of self-organization in nonequilibrium processes [4] and therefore their study transcends the limits of physics and chemistry and applies also to areas such as biology [5] or economics [6].

Whereas a great variety of reaction models has been considered—describing, for instance, chemical, nuclear, or birth-death events—the transport mechanisms taken into account have been mainly restricted to diffusion processes. Reaction-diffusion mathematical models have been proposed by modifying *ad hoc* the diffusion equation, introducing appropriate density dependent source terms. The typical form of the reaction-diffusion equation for a single species system is

$$\partial_t n - D\nabla^2 n = F(n), \quad (1)$$

where  $n(\mathbf{r}, t)$  is the species density,  $D$  is its diffusivity, and  $F(n)$  describes the reaction processes. For chemical reactions, this function is usually taken to reproduce the source terms in the corresponding rate equations of spatially homogeneous chemical kinetics. Although reaction-diffusion equations are proposed heuristically, their construction can be justified to some extent in the frame of microscopic or mesoscopic kinetic models [7].

Much work was devoted to the study of the mathematical properties of equations such as (1) [8], as well as to their application to real systems [4,5,9]. Their success in reproducing the complex evolution of such systems is indeed impressive. On the other hand, in spite of their relevance in some applications, the study of reacting sys-

tems where transport cannot be completely described by diffusion has received relatively little attention.

A convenient way to incorporate convective transport to a diffusing species consists in superposing to diffusion a given velocity field  $\mathbf{v}(\mathbf{r}, t)$ . In mathematical terms, this is achieved by adding a convection term  $\nabla \cdot (n\mathbf{v})$  to the diffusion operator on the left-hand side of Eq. (1). In the absence of reaction events, convection is known to drastically modify diffusive transport, giving place to mean square displacements which vary with time as  $\langle x^2 \rangle \sim t^\alpha$ , with  $\alpha \neq 1$  [10]. When reaction processes are considered, convection can strongly affect the stability of nonequilibrium patterns associated with the reaction-diffusion underlying system [11]. Even when diffusion is completely neglected, particles can be thought of as driven by the velocity field, and their motion can be consequently calculated. Within this approach, much effort has been devoted to the simulation of realistic velocity fields for complex flows, as in turbulence [12].

However, all these formulations for reacting and convecting fluids treat the density of reacting particles as a passive scalar, in the sense that they do not take into account the effect of reaction on transport but consider that the reacting particles are merely transported by the velocity field. In this paper, instead, we are interested in studying the full interplay of reaction and transport processes for convecting fluids, as usually done for diffusing systems. Therefore, we shall consider the more realistic situation in which the whole fluid is involved in reactions, so that these events not only modify the density as a passive scalar but—through their influence on the density—they affect also the evolution of other hydrodynamical fields, namely, the fluid velocity and the temperature.

The ultimate aim of our work consists in describing the evolution of an arbitrary set of chemical species actively involved in transport and reaction processes. This is a relevant problem associated, for instance, with atmospheric dynamics [13] and with nonstationary experi-

ments on chemical kinetics [14], where macroscopic fluid motion—due to stirring, convection, or simply the kinetics of the involved reactions—naturally occurs. Particularly important situations related to those systems concern combustion phenomena [15], shock waves in reacting fluids [16], and the evolution of charged diluted gases, such as plasmas or electronic and ionic beams [17].

This approach, however, requires us to treat simultaneously the evolution of the whole set of relevant hydrodynamical fields and therefore it constitutes a rather difficult mathematical problem. Thus, as a first step in its solution, we shall describe the relatively simple situation of a reacting perfect fluid interacting with a background host medium through mechanical and chemical processes. The effect of reactions will be added to the hydrodynamical equations in the same spirit used to propose reaction-diffusion equations such as Eq. (1). We shall mainly focus attention on the consequences of the strong interaction of reactions and transport involved in the model, analyzing the appearance of nonequilibrium structures in some particular situations. A numerical scheme for simulation of the system will be presented and we shall compare numerical results with our analytical calculations.

This paper is not supposed to contain an exhaustive analysis of reacting fluid dynamics or to refer to particular experimental situations, but to present a preliminary approach to this very wide problem in the frame of some reasonable simplifying assumptions, along the lines used in the study of reaction-diffusion systems. The relevant results obtained in this latter area suggest that reacting and convecting fluids deserve to be thoroughly analyzed.

## II. MODEL

Consider a fluid immersed in a host medium whose hydrodynamical state—characterized by homogeneous density, vanishing mean velocity, and constant temperature  $T_0$ —is not affected by the evolution of the guest fluid. This condition is met if, relative to the immersed fluid, the host medium can be thought of as a very dense gas of heavy particles [18]. The guest fluid is considered to be perfect, in the sense that it is in local thermal equilibrium. Thus, in the absence of the host medium, its hydrodynamical state would be governed by Euler continuity equations [19].

Guest-host interaction consists basically of mechanical and chemical processes. The former correspond to momentum and energy exchange which, at the hydrodynamical description level, translate into a relaxation of the velocity  $\mathbf{u}(\mathbf{r}, t)$  and the temperature  $T(\mathbf{r}, t)$  of the guest fluid toward those of the background gas. Such relaxation processes can be modeled at various levels of sophistication. Here they will be described by linear terms in the evolution equations for velocity and temperature. In this approximation—which at the kinetic description level can be justified in the frame of Bhatnagar-Gross-Krook models [20]—we describe velocity relaxation by a sort of “friction” term in the linear momentum balance  $-\gamma\mathbf{u}$ , whereas a formally analogous term  $-\lambda(T-T_0)$  stands for temperature relaxation in the energy balance.

Here we shall consider that chemical reactions affect only the number density  $n(\mathbf{r}, t)$  of the guest fluid. Indeed, individual reaction processes are not expected to modify the macroscopic fluid velocity  $\mathbf{u}$ . Furthermore, for the sake of simplicity in this first approach, we do not take into account chemical thermal effects. These could, however, be easily incorporated into the model at a further step. Thus reaction processes can be modeled as a source term in the density continuity equation, as a function  $F(n)$ , which in general depends on the fluid density. Other relevant quantities, such as reaction constants and the background density, enter  $F(n)$  as control parameters. This kind of approach is the usual one when considering reacting and diffusing systems [1].

Within this model, Euler continuity equations for a force-free fluid can be written as

$$\begin{aligned}\partial_t n + \nabla \cdot (n\mathbf{u}) &= F(n), \\ \partial_t \mathbf{u} + (\mathbf{u} \cdot \nabla)\mathbf{u} &= -\rho^{-1}\nabla p - \gamma\mathbf{u}, \\ \partial_t T + \mathbf{u} \cdot \nabla T &= -\frac{2}{d}T\nabla \cdot \mathbf{u} - \lambda(T - T_0).\end{aligned}\quad (2)$$

Here  $\rho = mn$  is the mass density, with  $m$  the mass of a fluid molecule, and  $d$  is the spatial dimension. For the perfect fluid, the pressure  $p$  is given by  $p = nkT$ , with  $k$  the Boltzmann constant.

In principle,  $\gamma$  and  $\lambda$  will be considered as constants. It is worthwhile to note that, given a specific guest-host interaction model at microscopic level, these two quantities are not independent. In fact, they can be calculated as mean values over the cross section characterizing the interaction. However, for the sake of generality, and since the present analysis is always developed at a macroscopic description level, we consider  $\gamma$  and  $\lambda$  as independent parameters.

According to the mass-action law of chemical kinetics,  $F(n)$  will typically be a polynomial in  $n$  [1], whose coefficients are given by the rate constants and the host medium density. For other reaction processes, however,  $F(n)$  could adopt a variety of forms [3,5]. Along with convective terms on the left-hand side of Eqs. (2), the source  $F(n)$  introduces nonlinearity in the problem.

For future reference, it is convenient to derive the evolution equation for the fluid pressure  $p = nkT$ . From Eqs. (2), we obtain

$$\begin{aligned}\partial_t p + \mathbf{u} \cdot \nabla p &= -\left(\frac{2}{d} + 1\right) p \nabla \cdot \mathbf{u} \\ &\quad - \lambda(p - nkT_0) + \frac{p}{n} F(n).\end{aligned}\quad (3)$$

Reaction processes do affect the evolution of pressure through the modification of the fluid density [cf. the term  $pF(n)/n$  in Eq. (3)].

The remainder of this paper is entirely devoted to the analysis of some basic phenomena associated with the model equations (2). Some of them, such as, for instance, wave fronts, have been suggested by numerical results obtained within the simulation scheme described in Sec. IV. Others, such as sound propagation, are standard steps in the study of ordinary fluid dynamics [19]. We shall pay particular attention to the combined effect of reaction and transport processes.

### III. BASIC PHENOMENOLOGY

In this section, we study analytically the model described by Eqs. (2). In the first place, we consider the hydrostatic state and its stability. This motivates also the study of sound propagation in the reacting fluid. Then, in the frame of some limiting cases, we analyze several nonequilibrium structures, which arise as a consequence of the complex interaction or reaction and transport.

#### A. Hydrostatics and sound propagation

In general, the hydrostatic state of a fluid is defined as a time independent state with vanishing velocity  $\partial_t \equiv 0$  and  $\mathbf{u} = 0$ . In Eqs. (2) this implies the following conditions:

$$F(n) = 0, \quad \nabla p = 0, \quad T = T_0. \quad (4)$$

Therefore, the hydrostatic state is spatially homogeneous, the fluid density is a root of the function  $F(n)$ , say  $n_0$ , and its temperature equals that of the host medium. The corresponding pressure is  $p_0 = n_0 k T_0$ . In contrast to the case of an ordinary fluid, the hydrostatic state is here well defined, as chemical reactions and guest-host interaction determine the values of density and temperature, respectively. Of course, such a state exists only if the reaction kinetics has a stationary solution, i.e., if  $F(n)$  has at least one root.

The stability analysis of the hydrostatic state in the linear approximation leads us to consider sound propagation in the fluid. Indeed, in an ordinary perfect fluid, infinitesimal perturbations around that state cause the relevant fields  $n(\mathbf{r}, t)$ ,  $\mathbf{u}(\mathbf{r}, t)$ , and  $T(\mathbf{r}, t)$  to oscillate around their equilibrium values, giving rise to sound waves which propagate without attenuation at a well-defined velocity  $c = \sqrt{(1 + 2/d)kT_0/m}$ .

In order to perform the linear stability analysis of the reacting fluid around its hydrostatic state, we suppose that density, velocity, and pressure differ from their equilibrium values  $n_0$ ,  $\mathbf{u}_0 = 0$ , and  $p_0$  in vanishingly small quantities, indicated by primes:

$$\begin{aligned} n(\mathbf{r}, t) &= n_0 + n'(\mathbf{r}, t), \\ \mathbf{u}(\mathbf{r}, t) &= \mathbf{u}'(\mathbf{r}, t), \\ p(\mathbf{r}, t) &= p_0 + p'(\mathbf{r}, t). \end{aligned} \quad (5)$$

Inserting these into Eqs. (2) and (3) and neglecting nonlinear terms in the perturbations, we get

$$\begin{aligned} \partial_t n' + n_0 \nabla \cdot \mathbf{u}' &= F'(n_0) n', \\ \partial_t \mathbf{u}' &= -\rho_0^{-1} \nabla p' - \gamma \mathbf{u}', \\ \partial_t p' &= -\left(\frac{2}{d} + 1\right) p_0 \nabla \cdot \mathbf{u}' - \lambda(p' - n' k T_0) \\ &\quad + n_0^{-1} p_0 F'(n_0) n'. \end{aligned} \quad (6)$$

Here  $F'$  indicates the derivative of  $F(n)$  with respect to  $n$  and  $\rho_0 = m n_0$ . As is usual when analyzing sound propagation [19], we have considered the evolution of pressure instead of that of temperature.

Plane sound waves are solutions to Eqs. (7) of the form

$$\begin{Bmatrix} n' \\ \mathbf{u}' \\ p' \end{Bmatrix} = \begin{Bmatrix} N \\ \mathbf{U} \\ P \end{Bmatrix} \exp[i(kx - \omega t)]. \quad (7)$$

In order that those equations have nontrivial solutions for the amplitudes  $N$ ,  $\mathbf{U}$ , and  $P$ ,  $k$  and  $\omega$  must satisfy a dispersion relation which we can write as

$$\begin{aligned} 0 &= i\omega^3 + [F'(n_0) - \gamma - \lambda]\omega^2 \\ &\quad + i[F'(n_0)(\gamma + \lambda) - \gamma\lambda - \omega_0^2]\omega \\ &\quad + \left[ \frac{\lambda\omega_0^2}{1 + 2/d} - \frac{F'(n_0)\omega_0^2}{1 + d/2} - F'(n_0)\gamma\lambda \right]. \end{aligned} \quad (8)$$

Here  $\omega_0 = ck$  is the frequency of a wave of wave number  $k$  in an ordinary perfect fluid, which moves at velocity  $c = \sqrt{(1 + 2/d)p_0/\rho_0}$ . In fact, for  $\gamma = \lambda = 0$  and  $F(n) \equiv 0$ , the solutions to Eq. (8) are the usual  $\omega = 0, \pm\omega_0$ .

When the frequencies  $\gamma$  and  $\lambda$ , and  $F'(n_0)$  do not vanish, Eq. (8) is a full third-degree polynomial equation for  $\omega$ , to be analyzed numerically. However, some general facts on its roots can be studied in an analytical way. In the first place, we have to observe that if  $F'(n_0) > 0$  the hydrostatic state is unstable, so that at least one of the solutions of Eq. (8) has a positive imaginary part. In fact, if the derivative of  $F(n)$  is positive at the equilibrium point  $n_0$ , it follows immediately that  $n_0$  is an unstable state of the homogeneous chemical kinetic equation  $\dot{n} = F(n)$ . Now, since neither spatial inhomogeneity nor velocity and temperature relaxation affect the local density so as to neutralize the effect of chemical reactions, none of these processes can change the unstable character of such an equilibrium point. Therefore, stable hydrostatic states—for which it makes sense to study the evolution of small perturbations in a linear approximation—are characterized by  $F'(n_0) < 0$ . Hereafter, we restrict the analysis to this case.

For  $\omega_0 \rightarrow 0$ , the three roots are pure imaginary numbers, with negative imaginary parts  $-\gamma$ ,  $-\lambda$ , and  $F'(n_0)$ . In this long-wavelength limit, then, the system is purely dissipative and no sound propagation occurs. Waves are overdamped by the relaxation of velocity and temperature and by chemical processes which tend to maintain the density in its equilibrium value  $n_0$ . This situation takes place up to a critical wave number  $k_c$ , at which the imaginary parts of a pair of roots, say  $\omega_1$  and  $\omega_2$ , collapse to a single value. From this point on, these two roots have the same (negative) imaginary part and their real parts are equal in modulus and opposite in sign. Meanwhile, the third root  $\omega_3$  is still purely imaginary. Thus, for wave numbers greater than the critical value, there is sound propagation with attenuation, caused again by mechanical interaction with the background and by reaction processes. For very large wave numbers, the real parts of  $\omega_1$  and  $\omega_2$  approach the values they would adopt in an ordinary perfect fluid, i.e.,  $\pm\omega_0$ . Their imaginary parts, as well as  $\omega_3$ , tend to constant finite values,

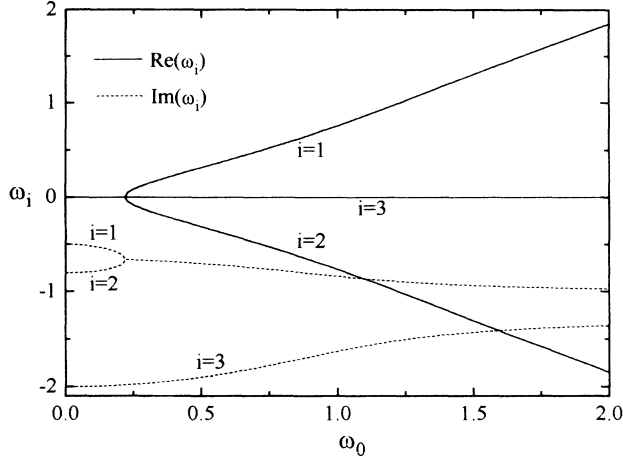


FIG. 1. Dispersion relation for sound propagation in the reacting fluid. This plot corresponds to the solution of Eq. (8), with  $F'(n_0) = -2$ ,  $\gamma = 0.5$ , and  $\lambda = 0.8$ , in three dimensions. Full and dashed lines respectively represent real and imaginary parts of the frequencies  $\omega_i$  as functions of the frequency of sound waves with the same wave number in a perfect ordinary fluid,  $\omega_0 = ck$ .

$$\begin{aligned} \text{Im}(\omega_{1,2}) &\rightarrow F'(n_0)/2(1 + 2/d) - \gamma/2 - \lambda/(2 + d), \\ \omega_3 &\rightarrow iF'(n_0)/(1 + d/2) - i\lambda/(1 + 2/d), \end{aligned} \quad (9)$$

for  $k \rightarrow \infty$ , and are therefore negligible with respect to the real parts of  $\omega_{1,2}$ . In this limit, sound propagation takes place in a time scale much shorter than attenuation, hence resembling the situation in an ordinary fluid.

Although it is difficult to obtain the critical wave number  $k_c$  analytically, it can be easily shown that it is of the order of  $c^{-1} \max(\gamma, \lambda)$ . As a consequence, if both  $\gamma$  and  $\lambda$  tend to zero, the purely dissipative region disappears. In this situation, sound propagation does occur for all values of  $k$  and the only attenuation effect comes from chemical processes, through density relaxation.

Figure 1 shows the real and imaginary parts of the solutions to Eq. (8), calculated for  $F'(n_0) = -2$ ,  $\gamma = 0.5$ , and  $\lambda = 0.8$ . This plot summarizes the typical behavior of the three roots, as  $\omega_0 = ck$  varies.

### B. Nonequilibrium structures in the isothermal frictionless limit

In contrast to the previous analysis, from now on we shall take into account the full nonlinear character of Eqs. (2), due both to the convection operator  $\mathbf{u} \cdot \nabla$  and to nonlinearity in  $F(n)$ . Therefore, in order to simplify the problem, we restrict hereafter the analysis to the case where the fluid temperature  $T(\mathbf{r}, t)$  equals that of the background  $T_0$ . This isothermal situation is met if temperature relaxation is fast enough, i.e., if  $\lambda \rightarrow \infty$ . In this limit, the only relevant hydrodynamical fields are density and velocity; the first two of Eqs. (2) reduce to

$$\begin{aligned} \partial_t n + \nabla \cdot (n\mathbf{u}) &= F(n), \\ \partial_t \mathbf{u} + (\mathbf{u} \cdot \nabla)\mathbf{u} &= -\frac{1}{2}v_0^2 \frac{\nabla n}{n} - \gamma\mathbf{u}, \end{aligned} \quad (10)$$

with  $v_0 = \sqrt{2kT_0/m}$ .

An interesting situation for studying Eqs. (10) is the limit  $\gamma \rightarrow 0$ . In this frictionless case, those equations admit spatially inhomogeneous stationary solutions. Such structures, whose existence would not be possible in an ordinary fluid, are a direct consequence of the interplay of reaction and transport. For small nonzero  $\gamma$ , the structures are expected to form and then decay towards a homogeneous state, due to velocity relaxation. For the sake of simplicity, we consider that the flow has plane symmetry along the  $x$  axis. Density and velocity satisfy then

$$\frac{d(nu)}{dx} = F(n), \quad (11)$$

$$u \frac{du}{dx} = -\frac{1}{2}v_0^2 \frac{dn}{dx},$$

with  $u = \mathbf{u} \cdot \hat{\mathbf{x}}$ . The second of these equations relates density and velocity according to

$$u = \pm v_0 \sqrt{\ln(n_0/n)}, \quad (12)$$

where the integration constant  $n_0$  can be identified with the density at the points where  $u = 0$ . The velocity is well defined if  $n_0 > n$  at every point, indicating that particles tend to accumulate in the regions with low values of  $u$ . The undetermination of its sign is due to the symmetry of spatial inversion.

Inserting Eq. (12) into the first of Eqs. (11) yields an autonomous equation for the spatial dependence of the density:

$$\frac{dn}{dx} = \pm v_0^{-1} \frac{\sqrt{\ln(n_0/n)}}{\ln(n_0/n) - 1/2} F(n). \quad (13)$$

In order to illustrate some typical features of this one-dimensional dynamical system, we show in Fig. 2 a graph of  $dn/dx$  as a function of  $n$ , for the case  $F(n) = (n_1 - n)(n_2 - n)(n_3 - n)$ . This particular choice of  $F(n)$  is motivated by the relevance that such a reaction model, namely, the Schlögl model [21], has had in the study of structure formation in reacting and diffusing systems [1,22]. For  $n_1 > n_2 > n_3$ , the corresponding spatially homogeneous evolutionary problem  $\dot{n} = F(n)$  has two stable equilibrium states  $n_1$  and  $n_3$  and an unstable one  $n_2$ . In the present problem, with  $n_0 > n_1$ , this bistable model exhibits all the typical characteristics of more general cases.

Consider first the loop labeled 1 in Fig. 2. It is delimited by the stable state  $n_1$  and a root of  $dn/dx$  at  $n_0$ . Note that this root appears whatever  $F(n)$  is. In fact, it is due to the zero of  $\ln(n_0/n)$  in the numerator of Eq. (13) for  $n \rightarrow n_0$ . Therefore, the behavior of  $dn/dx$  near  $n_0$  is independent of the reaction model. The loop represents a stationary solution which for  $x \rightarrow \pm\infty$  asymptotically approaches the stable state  $n_1$ . In intermediate regions it has a bump at whose maximum the density attains the value  $n_0$ . At the maximum the velocity vanishes and it

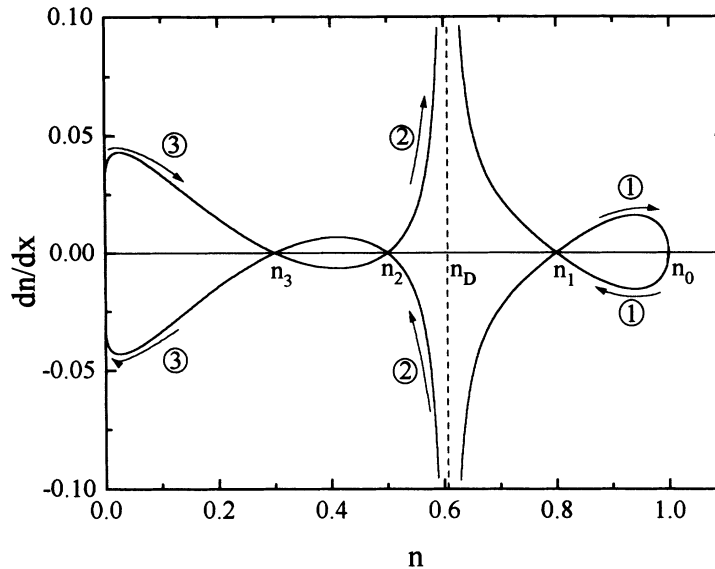


FIG. 2. Spatial derivative of the density  $n(x)$  as a function of  $n$  for a stationary, isothermal, frictionless fluid with planar symmetry, from Eq. (13). The reaction function is  $F(n) = (n_1 - n)(n_2 - n)(n_3 - n)$  with  $n_1 = 0.8$ ,  $n_2 = 0.5$ , and  $n_3 = 0.3$ . The density at the points where velocity vanishes is  $n_0 = 1$ . Arrows and labels inside circles refer to the solutions analyzed in Sec. III B.

is positive at the left and negative at the right. As a natural consequence of this flux toward the bump, particles accumulate continuously. This accumulation, however, is limited by a reaction which induces the density to approach the stable value  $n_1$ . It is precisely this competition of reaction and transport processes which gives rise to this nonequilibrium structure.

The fact that in this solution the density approaches the stable value  $n_1$  for large  $|x|$  suggests that it is a stable structure. This seems to be supported by the numerical simulations described in Sec. IV.

It can be shown from Eq. (13) that near the bump maximum the density behaves as

$$n(x) \approx n_0 \left[ 1 - \left( \frac{F(n_0)}{v_0 n_0} \right)^2 (x - x_1)^2 \right], \quad (14)$$

where  $x_1$  is the position of the maximum. The bump width is then determined by the reaction function  $F(n)$  evaluated at the maximum and by the temperature, through the velocity  $v_0$ . If  $n_1$  and  $n_0$  are near enough,  $F(n)$  can be approximated by a linear function for  $n_1 < n < n_0$ ,  $F(n) \approx F'(n_1)(n - n_1)$ . In such case, it is possible to find the complete solution to Eq. (13). It reads

$$n(x) = n_0 \left\{ 1 + \epsilon \tanh^2 \left[ \frac{\sqrt{\epsilon} F'(n_1)}{v_0} (x - x_1) \right] \right\}^{-1}, \quad (15)$$

with  $\epsilon = n_0/n_1 - 1$ . A schematic representation of this solution is labeled 1 in Fig. 3.

The spatial derivative of  $n$  in Eq. (13) diverges at  $n_D = n_0 \exp(-1/2)$ . Again, this is a feature independent of the reaction model and can be expected to occur whatever  $F(n)$  is. Associated with this divergence is a series of singular solutions, one of which is labeled 2 in Fig. 2. In this solution, the density approaches one of the stationary states as  $x \rightarrow \pm\infty$  and for finite  $x$  it has a symmetric

peaked structure, attaining  $n_D$  at the maximum. It is schematically shown in Fig. 3 as curve 2. From Eq. (13), it can be shown that, near the peak, the density behaves as

$$n(x) \approx n_D \left[ 1 - \sqrt{\frac{2^{1/2} F(n_D)}{v_0 n_D}} |x - x_2| \right], \quad (16)$$

where  $x_2$  is the position of the peak. Again, the width of this structure is determined by the reaction model and the temperature of the host medium.

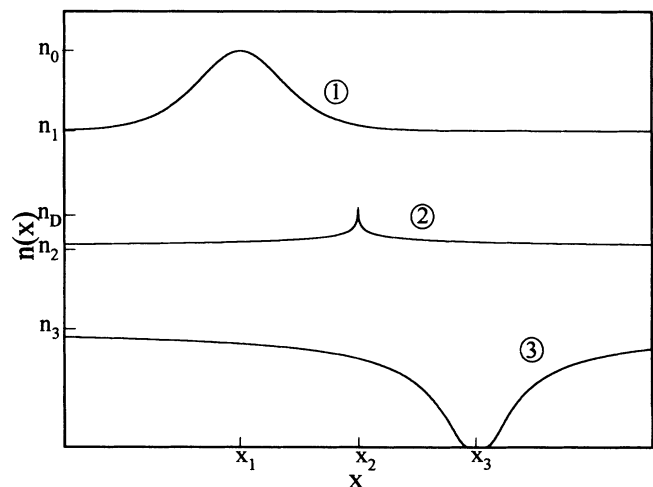


FIG. 3. Stationary density profiles for an isothermal frictionless fluid with planar symmetry. Labels inside circles refer to the corresponding curves of Fig. 2. These solutions reach their extremal points at  $x_1$ ,  $x_2$ , and  $x_3$ , respectively.

In this solution the velocity is discontinuous at  $x_2$ . Its values just at each side of the peak are finite, with the same modulus and opposite sign. The interaction dynamics of reaction and transport is therefore similar to the case analyzed before: the velocity field tends to accumulate particles at the peak, but chemical processes attenuate such accumulation by “removing” those particles. In the case shown in Fig. 2, this structure is not expected to be stable. Indeed, the asymptotic value  $n_2$  is an unstable equilibrium for the density and even an infinitely small perturbation would take off the system from that state. However, a structure of the same type should become stable if the divergence at  $n_D$  is associated with a stable equilibrium point, for instance, if  $n_D$  is situated just above  $n_3$ . In that case, such a structure—characterized by the discontinuity in the velocity field—could be generated by collision of two shock fronts of the type analyzed numerically in Sec. IV.

A third structure associated with a feature in  $dn/dx$  and independent of the reaction model is labeled 3 in Fig. 2. In this case, the density vanishes at  $x_3$  and, around this point, there is a zone of density depletion. The minimum at  $x_3$  is due to the inverse logarithmic behavior of the spatial derivative of the density near the origin  $dn/dx \sim 1/\sqrt{-\ln n}$ . It is not possible to obtain the explicit form of  $n(x)$  near  $x_3$ , but we find that

$$n\sqrt{-\ln n} - \frac{\sqrt{\pi}}{2} \left[ \operatorname{erf}(\sqrt{-\ln n}) - 1 \right] \approx v_0^{-1} |F(0)| |x - x_3|, \quad (17)$$

with  $\operatorname{erf}(z)$  the error function. In the case shown in Fig. 2, the density approaches the stable value  $n_3$  as  $x \rightarrow \pm\infty$  so that, according to the arguments applied before, this structure would be stable. It is schematically shown as curve 3 in Fig. 3.

In this solution, the velocity is negative at the left and positive at the right of the depletion zone. Thus reaction and transport here interchange the roles they played in the cases studied before. In fact, due to the divergent character of the velocity field, particles are continuously removed from the region near  $x_3$ , but, since  $n = 0$  is a nonequilibrium state of the reaction processes, new particles are “created” at the depletion zone. Again, the competition between reaction and transport is responsible for the existence of this nonequilibrium structure.

Other inhomogeneous solutions to Eqs. (11) are the ones connecting two different equilibrium states, approached as  $x \rightarrow \pm\infty$ , respectively. For instance, in Fig. 2, two of these solutions are represented by the curved segments ending at  $n_3$  and  $n_2$ . However, for continuous  $F(n)$ , among two neighbor equilibrium points, one is stable and the other unstable, so that a structure connecting both states is expected to be unstable. Besides this, in such cases, the effect of transport is negligible as the solution is mainly determined by the form of the reaction function  $F(n)$ . From the point of view of the interplay of transport and reaction, therefore, those cases are uninteresting.

Marginal situations, such as structures that eventually appear when one of the roots of  $F(n)$  coincides precisely

with the points at which  $dn/dx$  is singular due to transport, namely  $n_0$ ,  $n_D$ , and  $n = 0$ , deserve further consideration.

Finally, it is worthwhile to stress that here we have treated the stability of stationary structures in a semi-qualitative way. A detailed study of this point would permit us to answer several important questions such as, for instance, if transport is able to stabilize a chemically unstable state and if so, to what extent.

### C. Wave fronts

Numerical simulations suggest that, when velocity relaxation does act ( $\gamma \neq 0$ ) and under fairly general conditions, a very common feature in the evolution of the perfect fluid with bistable chemical processes is the development of wave fronts. These S-shaped structures, which connect two regions where the density equals one of its stable values, move at a well-defined velocity.

In order to obtain an analytical description of these wave fronts, consider a solution to the one-dimensional version of Eqs. (10) in which both the density and the velocity field depend on space and time through the combination  $\xi = x - ct$ , with  $c$  a constant, so that  $n(x, t) \equiv n(x - ct)$  and  $u(x, t) \equiv u(x - ct)$ . If it exists, such a solution would represent a shape-preserving wave moving with velocity  $c$ . In this situation, Eqs. (10) reduce to

$$\begin{aligned} (u - c)n' + nu' &= F(n), \\ v_0^2 n' / 2n + (u - c)u' &= -\gamma u, \end{aligned} \quad (18)$$

where primes indicate differentiation with respect to  $\xi = x - ct$ . This set of ordinary differential equations is equivalent to the two-dimensional dynamical system

$$\begin{aligned} n' &= \frac{F(n)(u - c) + \gamma nu}{(u - c)^2 - v_1^2}, \\ u' &= -\frac{v_1^2 F(n) + \gamma nu(u - c)}{n[(u - c)^2 - v_1^2]}, \end{aligned} \quad (19)$$

with  $v_1^2 = v_0^2/2 = kT_0/m$ .

The equilibrium points of Eqs. (19), defined by  $n' = 0$  and  $u' = 0$ , correspond to  $u = 0$  and  $F(n) = 0$ . As before, we consider that  $F(n)$  has three roots  $n_1$ ,  $n_2$ , and  $n_3$  such that  $n_1 > n_2 > n_3$ ,  $n_1$  and  $n_3$  being stable equilibria of the spatially homogeneous problem  $\dot{n} = F(n)$ . A wave front connecting the two stable states  $n_1$  and  $n_3$  is a solution to Eqs. (19) which asymptotically approaches one of those states for  $\xi \rightarrow -\infty$  and the other for  $\xi \rightarrow +\infty$ . This situation is usually met when both  $(n, u) = (n_1, 0)$  and  $(n, u) = (n_3, 0)$  are unstable equilibrium points of the dynamical system (19) such that the corresponding eigenvalues are real and opposite in sign. In this situation, the wave front solution corresponds in the phase portrait of Eqs. (19) to an unstable manifold of one of the unstable points which exactly connects with a stable manifold of the other (see Fig. 4).

The eigenvalues of the dynamical system (19) at  $(n, u) = (n_i, 0)$  equal

$$\mu = \frac{c[F'(n_i) - \gamma] \pm \sqrt{c^2[F'(n_i) - \gamma]^2 - 4\gamma F'(n_i)(v_1^2 - c^2)}}{2(v_1^2 - c^2)}. \quad (20)$$

Taking into account that at the equilibrium points  $n_1$  and  $n_3$  we have  $F'(n_i) < 0$ , it is easily seen that the eigenvalues have opposite signs only if  $-v_1 < c < v_1$ . This implies that, as we could expect, the maximum velocity for the wave front is of the order of the thermal velocity  $|c| < \sqrt{kT_0/m}$ .

A numerical analysis of Eqs. (19) shows that the connection of the manifolds of the equilibrium points occurs for a well-defined, unique value of  $c \in (-v_1, v_1)$ . This is precisely the wave front velocity. When  $c$  adopts that value, the dynamical system phase portrait is of the type schematically shown in Fig. 4 for the case  $c > 0$ . The dotted line represents the connected manifolds between  $(n_1, 0)$  and  $(n_3, 0)$ . The upper-right plot shows a scheme of the wave front density and velocity as functions of  $\xi$ . In this graph, the arrow indicates the motion direction of the front. Observe that in this case  $(n_2, 0)$  is a stable equilibrium point with complex eigenvalues.

A semiquantitative evaluation of the wave front velocity, which suggests the dependence of  $c$  on the external parameters and moreover provides an estimation of the wave front width, can be outlined as follows [22]. Let  $n_-$  and  $n_+$  be the asymptotic density values at the left and the right of the wave front, respectively. Integrating the first of Eqs. (18) with respect to  $\xi$  in the whole interval yields

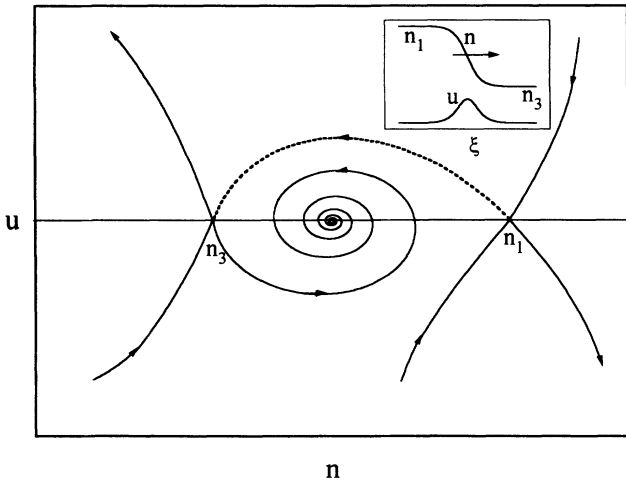


FIG. 4. Schematic representation of the phase portrait for the dynamical system Eq. (19), with the precise value of the parameter  $c (> 0)$  such that a wave front solution connecting the stationary stable states  $n_1$  and  $n_3$  exists. Arrows indicate the flow in the phase plane and the dashed line represents the wave front solution. In the upper-right graph, this solution is schematically plotted as a function of the similarity variable  $\xi = x - ct$ , along with the velocity profile  $u(\xi)$ . The wave front moves from left to right, as indicated by the arrow.

$$-c(n_+ - n_-) = \int_{-\infty}^{+\infty} F(n) d\xi = \int_{n_-}^{n_+} \frac{F(n)}{dn/d\xi} dn \approx \frac{\Delta}{n_+ - n_-} I, \quad (21)$$

where  $\Delta$  is the width of the wave front and  $I$  is the integral of  $F(n)$  with respect to  $n$ , between  $n_-$  and  $n_+$ . Assuming then that the point at which the density equals  $n_2$  coincides approximately with the velocity maximum, the same equation provides an evaluation for the maximum value of the velocity field at the wave front:  $u_{\max} \approx c$ . Taking this into account and integrating the second of Eqs. (18) with respect to  $\xi$ , we obtain

$$-K\gamma c\Delta \approx v_1^2 \ln(n_+/n_-), \quad (22)$$

where  $K$  is a factor of the order of unity, which depends on the shape of the velocity profile. Note that since  $\Delta$  is a positive quantity, this equation implies that  $c$  and  $\ln(n_+/n_-)$  are opposite in sign. In other words, if  $n_+ = n_3$  and  $n_- = n_1$ , the velocity is positive and vice versa. As a consequence, the wave front moves always “forward”—as indicated in the upper-right graph of Fig. 4—and the domain with higher density  $n_1$  advances always over the lower one. This conclusion is widely supported by numerical simulations.

Combining Eqs. (21) and (22) we get

$$c^2 \approx \frac{v_1^2 I \ln(n_+/n_-)}{K\gamma (n_+ - n_-)^2} \quad (23)$$

and

$$\Delta^2 \approx \frac{v_1^2}{IK\gamma} (n_+ - n_-)^2 \ln(n_+/n_-). \quad (24)$$

These two quantities are well defined if the integral  $I$  and  $\ln(n_+/n_-)$  have the same sign. This is a nontrivial condition on the reaction function  $F(n)$  for the wave front solution to exist. It implies that the integral of  $F(n)$  between  $n_2$  and  $n_1$  must exceed the absolute value of the integral between  $n_3$  and  $n_2$ . In this sense, the higher stable state  $n_1$  must be more “weighty” than  $n_3$  with respect to the intermediate  $n_2$ . This is in agreement with the fact that the higher stable state dominates the lower one, as the wave front moves.

For given values of  $n_-$  and  $n_+$ , as far as the wave front exists,  $(n_2, 0)$  is a stable point of the dynamical system (19). According to the above discussion, if the parameter  $c$  in Eqs. (19) is varied so as to change its sign, the wave front solution ceases to exist. It can be shown that, at the same time,  $(n_2, 0)$  becomes unstable. Numerical analysis of the dynamical system indicates that, in this situation, a limit cycle appears at infinity and shrinks towards  $(n_2, 0)$  as the modulus of  $c$  increases. Figure 5 shows this limit cycle in the phase plane  $(n, u)$  and the small graphs

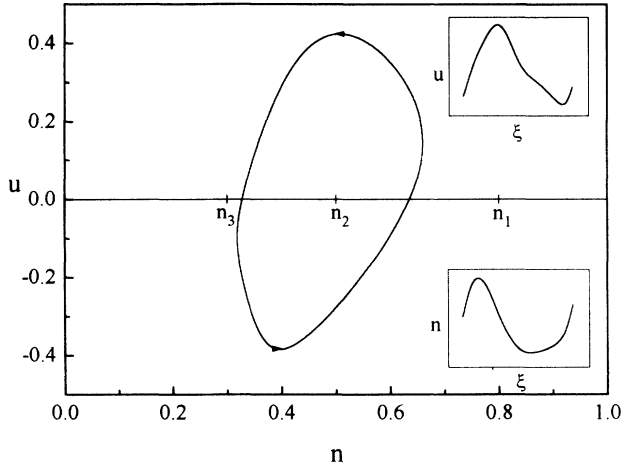


FIG. 5. Limit-cycle solution of the dynamical system Eq. (19) in the phase plane  $(n, u)$ . The small plots represent the density profile  $n(\xi)$  and the velocity profile  $u(\xi)$  as functions of the similarity variable  $\xi = x - ct$ , along a whole period in the limit cycle.

depict the dependence of density and velocity on  $\xi$  along a whole cycle period. This solution represents a train of density crests moving at constant velocity. As the wave front studied above, this is a shape-preserving nonlinear wave originating in a strong competition between reaction and transport. As discussed previously, by “creating” or “annihilating” particles, chemical processes compensate local depletion or overpopulation caused by the flow.

#### IV. NUMERICAL MODEL

##### A. Simulation scheme

The simulation scheme used to study the reacting perfect fluid from a numerical viewpoint is based on discrete velocity kinetic models with reactions [23,24] and can be seen as a variation of cellular automata methods [25] or of the lattice Boltzmann equation formulation [26]. In this three-velocity model, which is intended to mimic a reacting fluid in the isothermal situation, the system evolves on a one-dimensional lattice at discrete time steps. The extension to more dimensions is straightforward. At a given time, three positive real numbers  $f_-(x, t)$ ,  $f_0(x, t)$ , and  $f_+(x, t)$  are defined on each lattice site. They stand for the distribution functions of particles with velocity  $v$ ,  $0$ , and  $-v$  ( $v = \text{const}$ ), respectively. These three distribution functions make it possible to define three independent “macroscopic” fields—density, velocity, and temperature—given by

$$\begin{aligned} n(x, t) &= f_-(x, t) + f_0(x, t) + f_+(x, t), \\ n(x, t)u(x, t) &= v[f_+(x, t) - f_-(x, t)], \\ n(x, t)kT(x, t)/m &= v^2[f_-(x, t) + f_+(x, t)] \\ &\quad - n(x, t)u(x, t)^2. \end{aligned} \quad (25)$$

Note that for a many-dimensional system the third of these equations would include a coefficient depending on the dimension.

The evolution of  $f_i(x, t)$  ( $i = -, 0, +$ ) is completely deterministic and, at each time step, consists of four substeps that occur successively. The first one describes reaction events and is associated with a time interval  $\delta t_R$ . In this substep the distribution functions are modified to

$$f_i(x, t + \delta t_R) = f_i(x, t) \frac{n(x, t) + F(n(x, t)) \delta t_R}{n(x, t)}, \quad (26)$$

where  $F(n)$  is the reaction function that appears in the first of Eqs. (2). This process is local in space, and the fact that  $f_i(x, t + \delta t_R)$  is proportional to  $f_i(x, t)$  ensures that velocity and temperature are not modified by reactions. Note that  $\delta t_R$  should be small enough to ensure positivity of the distribution functions.

The second substep stands for particle transport. The associated time interval  $\delta t_T$  is related to the lattice spacing  $\delta x$  by  $\delta x = v\delta t_T$ . In this substep distribution functions at neighbor sites are interchanged according to the fluid motion:

$$\begin{aligned} f_0(x, t + \delta t_T) &= f_0(x, t), \\ f_{\pm}(x, t + \delta t_T) &= f_{\pm}(x \mp \delta x, t). \end{aligned} \quad (27)$$

The fact that this process preserves positivity is obvious.

Velocity relaxation is described by the third substep. It is supposed that this local process must preserve density and temperature, whereas velocity is modified to a lower value  $u \rightarrow u(1 - \Gamma)$ , with  $0 < \Gamma < 1$ . Here  $\Gamma$  can be related to the friction coefficient  $\gamma$  [cf. the second of Eqs. (2)] by means of the time interval  $\delta t_U$  associated with this substep  $\Gamma = \delta t_U \gamma$ . The distribution functions are modified according to

$$\begin{aligned} f_0(x, t + \delta t_U) &= f_0(x, t) + \Gamma(2 - \Gamma) n(x, t)u(x, t)^2/v^2, \\ f_{\pm}(x, t + \delta t_U) &= f_{\pm}(x, t) - \Gamma(2 - \Gamma) n(x, t)u(x, t)^2/2v^2 \\ &\quad \mp \Gamma n(x, t)u(x, t)/2v. \end{aligned} \quad (28)$$

It can be shown that, as far as  $0 < \Gamma < 1$ ,  $f_i(x, t + \delta t_U)$  is always positive.

Finally, the fourth substep describes the local thermalization of the fluid. At this point, the distribution functions are modified in such a way that density and velocity remain invariant and temperature changes to  $T_0$ , the host medium temperature. This substep, whose associated time interval  $\delta t_0$  is irrelevant to the dynamics, is defined by

$$\begin{aligned} f_0(x, t + \delta t_0) &= n(x, t)[1 - u(x, t)^2/v^2 - kT_0/mv^2], \\ f_{\pm}(x, t + \delta t_0) &= n(x, t)[kT_0/mv^2 + u(x, t)^2/v^2 \\ &\quad \pm u(x, t)/v]/2. \end{aligned} \quad (29)$$

Unfortunately, it is impossible to ensure here that  $f_i(x, t + \delta t_0)$  will be positive. The analysis of Eqs. (29) for  $0 < kT_0/mv^2 < 1$  and  $-1 < u(x, t)/v < 1$ , which are the admissible values for temperature and velocity, indicates that the distribution functions can become negative, especially when  $T_0$  is near one of its extreme values. In any

case, for a given value of  $T_0$ , there are always at least two velocity intervals for which either  $f_0$  or  $f_{\pm}$  change their sign. Since the invariance of local density and velocity is required by mass and momentum conservation in the guest-host interaction, it is necessary to sacrifice the efficiency of thermalization. Therefore, if a sign change will occur, the value of the corresponding distribution function is automatically set equal to zero and the others are adjusted to preserve density and velocity. This implies a difference between the resulting temperature and  $T_0$ . Although this discrepancy is unavoidable, it can be minimized by a convenient choice of  $T_0$ . It can be seen that its optimal value is  $kT_0/mv^2 = 1/4$ .

It is worthwhile to stress that this numerical scheme does not include interactions, i.e., binary collisions, between fluid particles. These interactions are indeed important in the evolution of a fluid, as they determine its microscopic state. In a perfect fluid, for instance, binary collisions are responsible for local thermodynamical equilibrium in the system. However, in the isothermal case considered here, local equilibrium is determined by the guest-host interaction, so that this process is supposed to prevail over other collision events. In other, more general situations these collision events should be taken into

account.

The four substeps described above, always applied in succession, constitute a whole time step of longitude  $\delta t = \delta t_R + \delta t_T + \delta t_U + \delta t_0$ . The relative strength of reaction and velocity relaxation with respect to transport and thermalization—which define their own rates—can be modified by changing the values of  $\delta t_R$  and  $\delta t_U$  or, alternatively, by changing  $F(n)$  and  $\Gamma$ .

Being a discrete velocity model, this simulation scheme is particularly suitable for numerical investigation of the reacting perfect fluid. It avoids the typical strong instabilities occurring in the discretization of the perfect fluid equations for their numerical solution. On the other hand, the simulation is not expected to reproduce in all detail the evolution of a real system of this type. Indeed, a three-velocity model can at most mimic in a semiquantitative manner the behavior of such a system. Therefore, results of simulations have to be seen as merely indicative of the features we could find in a more realistic situation. Nevertheless, as said before, we detected many of the structures analyzed in Sec. III for Eqs. (2) in numerical simulations.

The simulation scheme outlined here exhibits a good overall performance, with some rare instabilities of neg-

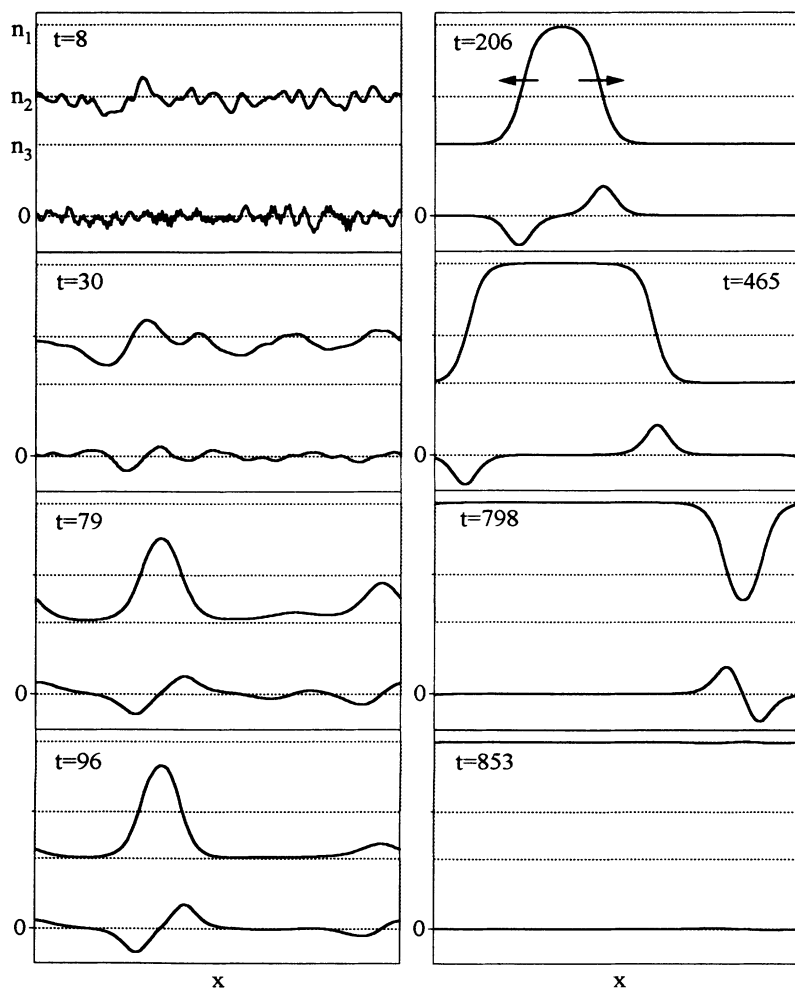


FIG. 6. Numerical simulation of the one-dimensional isothermal reacting fluid, with friction coefficient  $\Gamma = 0.03$ , temperature  $kT_0/mv^2 = 0.25$ , and periodic boundary conditions. The reaction function is  $F(n) = (n_1 - n)(n_2 - n)(n_3 - n)$  with  $n_1 = 0.8$ ,  $n_2 = 0.5$ , and  $n_3 = 0.3$ . In each plot, the upper curve represents the density profile as a function of position and the lower one is the corresponding velocity profile. The initial condition was chosen at random, so that density fluctuates around the unstable equilibrium state  $n_2$  and the average velocity vanishes. Time is indicated in units of  $\delta t$ .

ligible effect in certain limit cases. In the next section, we present some representative simulation results.

### B. Numerical results

Numerical simulations have been performed on a 200-site lattice with  $\delta x = 1$  and periodic boundary conditions for a fluid with  $v = 1$ . The reaction model was given by the function  $F(n) = (n_1 - n)(n_2 - n)(n_3 - n)$  with  $n_1 = 0.8$ ,  $n_2 = 0.5$ , and  $n_3 = 0.3$ , and the reaction interval  $\delta t_R$  has been chosen equal to one. According to the discussion above, we fixed the background temperature so that  $kT_0/mv^2 = 0.25$ . We have always chosen the initial condition at random, in such a manner that the initial density  $n(x, 0) = \sum_i f_i(x, 0)$  fluctuated around the unstable equilibrium state  $n_2$ .

Figure 6 shows a typical realization run with  $\Gamma = 0.03$ . In each plot, the upper curve corresponds to density and the lower one to velocity. During the first evolution steps ( $t \lesssim 30 \delta t$ ) initial fluctuations are rapidly smoothed out, due to velocity and temperature relaxation. At  $t \approx 100 \delta t$  only two density bumps persist, with similar velocity profiles. In the remainder of the spatial domain, the density has relaxed toward the lower stable state  $n_3$  and velocity has practically vanished. The density maximum in the rightmost bump is below the unstable state  $n_2$ , indicating that this structure is a candidate to disappear under the cooperative action of chemical processes—which makes the density approach  $n_3$ —and of its velocity field—which tends to deplete the region.

In the other bump, instead, density is definitely above  $n_2$  and therefore depletion due to transport must compete with reactions which tend to increase density. Eventually, reactions prevail and two opposite wave fronts form at  $t \gtrsim 200 \delta t$ . These are precisely the type of wave fronts studied at the end of Sec. III (cf. Fig. 4). They move at a velocity  $c \approx \pm 0.115 \delta x / \delta t$  and have a width of about  $40 \delta x$ . As time elapses, due to the periodic boundaries in the simulation, the fronts are led to collide and annihilate each other. The depleted region in between is filled and, finally, the density reaches a homogeneous state at the upper stable equilibrium value, with vanishing velocity. At  $t = 853 \delta t$  (see Fig. 6), this state has practically been established.

Figures 7 and 8 correspond to simulations in the frictionless case  $\Gamma = 0$ . The first one is the numerical version of the bump described in Sec. III and labeled 1 in Fig. 3. It is plotted at  $t = 235 \delta t$  and originated from a random initial density with mean value slightly above  $n_2$ . Two fronts have formed and then collided, and their collision produced a local overpopulation which rapidly relaxed to this very stable structure. Strictly speaking, although it can last for a long time almost unperturbed, in this numerical simulation such a structure will finally disappear. This is due to periodic boundary conditions, which establish an interaction between the bump and its images in the remainder of the “infinite” spatial domain.

This effect is also apparent in the velocity field. In fact, in a strictly infinite domain,  $u$  should approach constant values as  $x \rightarrow \pm\infty$ . These asymptotic values, equal

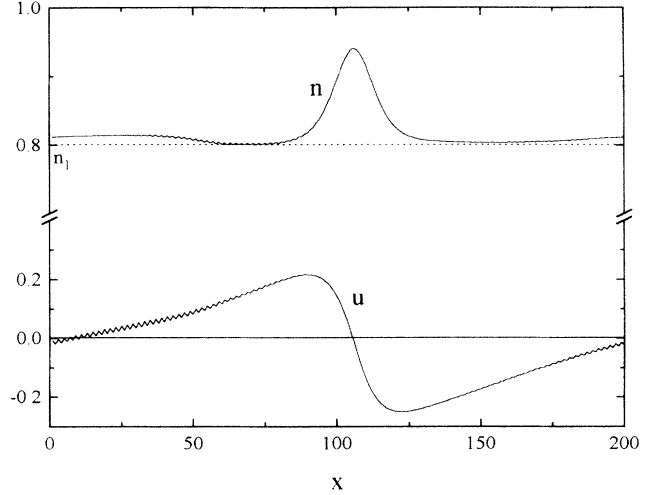


FIG. 7. Numerical simulation of the one-dimensional isothermal frictionless fluid, with temperature  $kT_0/mv^2 = 0.25$  and periodic boundary conditions. The reaction function and the initial condition are the same as in Fig. 6. Curves represent the density and the velocity profiles as a function of position at time  $t = 235 \delta t$ . A bump of the type labeled 1 in Fig. 3 has formed. Note the small oscillations due to numerical instabilities.

in modulus and opposite in sign, are given by  $u(n_1)$  in Eq. (12). In the periodic domain, instead,  $u(x, t)$  is a continuous function of  $x$  whose ends must connect with each other. Consequently, the velocity becomes negative to the left of the bump and positive to the right. This depletion in  $u(x, t)$  makes the velocity profile unable to

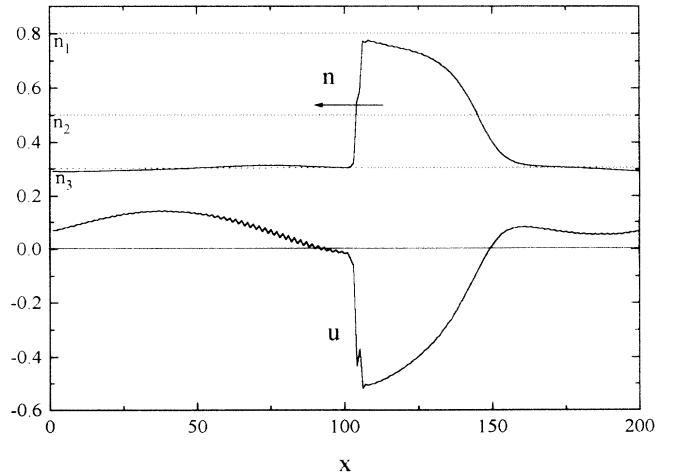


FIG. 8. Numerical simulation of the one-dimensional isothermal frictionless fluid in the same conditions as in Fig. 7, with a different random initial condition, at time  $t = 185 \delta t$ . A shock wave has developed and it proceeds from right to left with a velocity which practically equals the microscopic velocity of the fluid particles. Note the rather inhomogeneous velocity profile in the zone where the density is nearly constant.

compete with reactions, and finally density relaxes toward the homogenous state  $n_1$ .

Note the small oscillations both in  $u(x, t)$  and  $n(x, t)$  near the zone where  $u = 0$ . They are due to numerical instabilities and do not represent an important interference to simulations, as they remain bounded at all times. Such oscillations disappear as soon as some friction is added and velocity relaxation acts.

Finally, Fig. 8 shows the result of the evolution of a random initial condition at  $t = 185\delta t$ . It represents a structure which could only be observed in the frictionless case. This is a shock wave, i.e., a discontinuity in the density and the velocity, moving at  $c \approx v$ . Such shock waves are very common features in the numerical evolution of the frictionless fluid. As a matter of fact, the collision of two of these structures gave place to the bump plotted in Fig. 7. They form spontaneously in zones with high velocity gradients and develop as they move. Typically, at one side of the discontinuity, the density equals  $n_3$  and the velocity vanishes, whereas on the other side  $n = n_1$  and  $u$  reaches a finite value. The wave moves always toward the region with  $n = n_3$ . From the numerical point of view these structures are particularly unstable. Note, for instance, the irregularities in the velocity front. Small oscillations also appear in  $u(x, t)$  just at the left of the front.

Besides the shock front developing at  $100 < x < 150$ , Fig. 7 displays another typical feature in the evolution of reacting fluids. For  $0 < x < 100$ , density is practically constant whereas velocity is considerably inhomogeneous. This is again a consequence of the interplay of reactions and transport: by virtue of reaction processes, which maintain density near the stable state  $n_3$ , the fluid can support a relatively high velocity gradient without exhibiting strong variations in its spatial distribution.

## V. SUMMARY AND CONCLUSIONS

In this paper, we have analyzed some of the features in the dynamics of a perfect fluid interacting with a host medium through mechanical and chemical processes. This interaction is modeled at the hydrodynamical description level by suitable terms in the continuity equations for density, velocity, and temperature. Reaction events, which are not supposed to modify velocity and temperature, enter the density equation in the form of a density-dependent source term, as is usually done when modeling reacting and diffusing systems [1]. On the other hand, mechanical processes such as momentum and energy interchange do affect velocity and temperature but leave density unchanged. We have represented such processes with linear relaxation terms in the respective continuity equations.

In contrast to diffusing systems—where the existence of a background is assumed by the definition of the underlying transport process—for a one-species reacting perfect fluid it is necessary to add *a fortiori* a host medium, able to become involved in chemical reactions. Indeed, a reacting isolated species could not undergo realistic

chemical processes. The guest-host fluid system is then the simplest nontrivial case in which convective transport and reactions can interact. Moreover, considering the guest-host chemical interaction without taking into account mechanical processes—which can be naturally done in diffusing systems—would here result in unrealistic models as well.

Here we considered this simple guest-host model as a first step in the study of nonpassive reaction-transport interplay in fluids. However, it is clear that the model can be straightforwardly extended to more complex situations, taking into account several fluid species as well as the more complex mechanical interaction and chemical reactions.

In the first place, we studied the hydrostatic state of the reacting fluid, which, in contrast to that of an ordinary fluid, is well defined. In fact, reactions fix the possible values of density and mechanical processes determine velocity and temperature to equal those of the background medium. Small perturbations of hydrostatic stable states led us to consider sound propagation in the reacting fluid. We obtained that dispersion and attenuation of sound waves appear as a consequence of both reaction and relaxation processes. Although as discussed before these two kinds of processes cannot occur separately, it has to be noted that reactions alone are able to introduce dispersion and attenuation in sound propagation. This fact, which is essentially due to the density relaxation implied by reaction events, should also be observed in other oscillatory phenomena occurring in fluids, such as, for instance, gravity waves [27].

For the sake of simplicity, in this first approach to our model, we have then restricted the analysis to the isothermal case in which the fluid temperature field identically equals the background temperature. This limit corresponds to an infinitely effective temperature relaxation and reduces the number of unknowns in the problem. Our interest was concentrated in the study of nonequilibrium structures arising from the interplay of reaction and transport. In the situation in which velocity relaxation is neglected, we obtained several time independent inhomogeneous solutions with planar symmetry, characterized by bounded zones of overpopulation or density depletion and supporting space dependent velocity fields. All these structures—whose existence would be impossible in an ordinary fluid—can be seen to originate in a basic competition process between reactions and transport. When velocity tends to accumulate particles in a certain region, such accumulation is limited by reactions which maintain density near the corresponding equilibrium values. On the contrary, if there is a zone where the velocity field is divergent so as to deplete the population there, reactions provide new particles which compensate for the depletion. When the two processes balance, nonequilibrium structures arise. These structures are expected to vary with time if velocity relaxation is taken into account, progressively approaching a homogeneous state.

A most important structure observed to exist for bistable reaction models consists of a wave front connecting zones with homogeneous density and velocity. These shape-preserving solutions exist only when certain con-

ditions on the reaction model are fulfilled, related to the fact that the stable state with greater density prevails over the other. They move forward always at a constant, well-defined velocity, in such a way that at a given point in space the density varies from the lower stable state to the upper one. This fact makes evident an important difference from the case of a diffusing system with bistable reaction. In fact, in this latter situation, wave fronts can move forward or backward depending on the details of the reaction model, such that either stable state can be dominant. In the case of a perfect fluid, instead, wave fronts always lead the system to approach a homogeneous state in which the density has its greatest stable value.

Although we have analyzed wave fronts in the particular situation of planar symmetry—analogue to a one-dimensional problem—these solutions are expected to describe the evolution of density domains in many-dimensional cases, as observed in reaction-diffusion systems [22]. For a bistable reaction model in which the typical relaxation times are lower than those corresponding to transport processes, the fluid should evolve toward a state constituted by domains of almost constant density, whose values are given by the reaction stable states. Such domains should then move governed by the reaction-transport interplay. When the reaction model permits the formation of wave fronts, i.e., when the upper stable state is dominant, these structures should represent the evolution of the domain walls and the system would finally tend to a homogeneous high density state.

The numerical scheme presented in Sec. IV has been developed to gain insight into the main qualitative features in the behavior of the reacting fluid. Here it has

been mainly used to detect the type of nonequilibrium structures we could expect to describe within an analytical approach. The scheme consists of a three-velocity one-dimensional deterministic model, particularly suitable for simulation purposes. Three velocities with at least two different moduli (0 and  $v$ , in our case) are necessary to define independent density, velocity, and temperature fields. Most of the lattice gas models used in numerical simulations of ordinary fluids, such as, for instance, the Broadwell model and some of its variations [28], consider that all the possible velocities have the same modulus and are therefore unable to account for thermal effects. In such models, in fact, conservation of particle number is equivalent to energy conservation so that density and temperature are not independent quantities. This fact must be taken into account in eventual generalizations of the reacting fluid discrete velocity models to many-dimensional cases.

Possible extensions of the model and the particular situations presented here—which surely deserve future consideration—are, for instance, the inclusion of viscous dissipation, heat transport, and boundary conditions; the study of thermal effects, potential, and rotational flows in two and three dimensions; and the influence of reaction processes on more complex flows, such as on turbulent ones. The preliminary results presented in this paper hold within some simplifying approximations which do not necessarily correspond to a specific experimental situation. However, they clearly suggest that such generalizations to more realistic cases could give origin to a rich variety of new phenomena associated with the interplay of reaction and transport.

- 
- [1] A.S. Mikhailov, *Foundations of Synergetics I* (Springer, Berlin, 1990).
- [2] Y. Kuramoto, *Chemical Oscillations, Waves and Turbulence* (Springer, Berlin, 1984).
- [3] Ya.B. Zeldovich et al., *Mathematical Theory of Combustion and Explosion* (Consultants Bureau, New York, 1985).
- [4] H. Haken, *Synergetics. An Introduction* (Springer, Berlin, 1978).
- [5] J.D. Murray, *Mathematical Biology* (Springer, Berlin, 1989).
- [6] R.R. Nelson and S.G. Winter, *An Evolutionary Theory of Economic Change* (Harvard University Press, Cambridge, MA, 1982); G. Silverberg, in *Technical Change and Economic Theory*, edited by G. Dosi et al. (Pinter, New York, 1988), p. 531.
- [7] R. Spigler and D.H. Zanette, *IMA J. Appl. Math.* **49**, 217 (1992); *Z. Angew. Math. Phys.* **44**, 812 (1993).
- [8] J. Smoller, *Shock Waves and Reaction-Diffusion Equations* (Springer, Berlin, 1983).
- [9] J.J. Tyson, *The Belousov-Zhabotinskii Reaction* (Springer, Berlin, 1976).
- [10] G.K. Batchelor, *J. Fluid Mech.* **95**, 369 (1979); R. Mauri and S. Haber, *SIAM J. Appl. Math.* **46**, 49 (1986); D. ben-Avraham, F. Leyvraz, and S. Redner, *Phys. Rev. A* **45**, 2315 (1992); H.S. Wio and D.H. Zanette, *Phys. Rev. E* **47**, 384 (1993).
- [11] E.A. Spiegel and S. Zaleski, *Phys. Lett.* **106A**, 335 (1984); C.R. Doering and W. Horsthemke, *Phys. Lett. A* **182**, 227 (1993).
- [12] R.H. Kraichnan, *Phys. Fluids* **13**, 22 (1970); *J. Fluid Mech.* **77**, 753 (1976); J.C.H. Fung et al., *ibid.* **236**, 281 (1992); A. Careta, F. Sagués, and J.M. Sancho, *Phys. Rev. E* **48**, 2279 (1993).
- [13] J. Duderstand and W. Martin, *Transport Theory* (Wiley, New York, 1979).
- [14] R. Kapral, in *Advances in Chemical Physics*, edited by I. Prigogine and S. Rice (Wiley, New York, 1981), Vol. 48.
- [15] *Combustion Modelling*, edited by B. Larroutourol (World Scientific, London, 1991).
- [16] J.N. Bradley, *Shock Waves in Chemistry and Physics* (Wiley, New York, 1962).
- [17] M. Mitchner and C.H. Kruger, Jr., *Partially Ionized Gases* (Wiley, New York, 1973).
- [18] D.H. Zanette, *Phys. Lett. A* **163**, 254 (1992).
- [19] D.J. Tritton, *Physical Fluid Dynamics* (Clarendon, Oxford, 1988).
- [20] C. Cercignani, *The Boltzmann Equation and its Applications* (Springer, New York, 1988).
- [21] F. Schlögl, *Z. Phys.* **253**, 147 (1972).
- [22] P.C. Fife, *J. Chem. Phys.* **64**, 854 (1976); *Mathematical Aspects of Reacting and Diffusing Systems*, Lecture Notes in Biomathematics Vol. 28 (Springer, Berlin, 1979).

- [23] D.H. Zanette, *Physica* **148A**, 288 (1988); **153A**, 612 (1988); *J. Phys. A* **26**, 5339 (1993).
- [24] R. Monaco and L. Preziosi, *Fluid Dynamic Applications of the Discrete Boltzmann Equation*, Series in Advances in Mathematics for Applied Sciences Vol. 3 (World Scientific, Singapore, 1991).
- [25] D.H. Zanette, *Phys. Rev. A* **46**, 7573 (1992).
- [26] G. McNamara and G. Zanetti, *Phys. Rev. Lett.* **61**, 2332 (1988); S. Succi, R. Benzi, and F. Higuera, *Physica D* **47**, 219 (1991).
- [27] L.D. Landau and E.M. Lifshitz, *Fluid Mechanics* (Pergamon, Oxford, 1987).
- [28] See, for instance, U. Frisch, B. Hasslacher, and Y. Pomeau, *Phys. Rev. Lett.* **56**, 1505 (1986), and references therein.